

Ultrafast absorption of intense x rays by nitrogen molecules

Christian Buth,^{1, 2, 3, 4, a)} Ji-Cai Liu (刘纪彩),^{1, 5} Mau Hsiung Chen (陳茂雄),⁶ James P. Cryan,^{2, 7} Li Fang (方力),⁸ James M. Glowina,^{2, 9} Matthias Hoener,⁸ Ryan N. Coffee,^{2, 10} and Nora Berrah⁸

¹⁾ *Max-Planck-Institut für Kernphysik, Saupfercheckweg 1, 69117 Heidelberg, Germany*

²⁾ *The PULSE Institute for Ultrafast Energy Science, SLAC National Accelerator Laboratory, Menlo Park, California 94025, USA*

³⁾ *Department of Physics and Astronomy, Louisiana State University, Baton Rouge, Louisiana 70803, USA*

⁴⁾ *Argonne National Laboratory, Argonne, Illinois 60439, USA*

⁵⁾ *Department of Mathematics and Physics, North China Electric Power University, 102206 Beijing, China*

⁶⁾ *Physics Division, Lawrence Livermore National Laboratory, Livermore, California 94550, USA*

⁷⁾ *Department of Physics, Stanford University, Stanford, California 94305, USA*

⁸⁾ *Department of Physics, Western Michigan University, Kalamazoo, Michigan 49008, USA*

⁹⁾ *Department of Applied Physics, Stanford University, Stanford, California 94305, USA*

¹⁰⁾ *The Linac Coherent Light Source, SLAC National Accelerator Laboratory, Menlo Park, California 94025, USA*

(Dated: 31 May 2012)

We devise a theoretical description for the response of nitrogen molecules (N_2) to ultrashort and intense x rays from the free electron laser (FEL) Linac Coherent Light Source (LCLS). We set out from a rate-equation description for the x-ray absorption by a nitrogen atom. The equations are formulated using all one-x-ray-photon absorption cross sections and the Auger and radiative decay widths of multiply-ionized nitrogen atoms. Cross sections are obtained with a one-electron theory and decay widths are determined from *ab initio* computations using the Dirac-Hartree-Slater (DHS) method. We also calculate all binding and transition energies of nitrogen atoms in all charge states with the DHS method as the difference of two self-consistent field calculations (Δ SCF method). To describe the interaction with N_2 , a detailed investigation of intense x-ray-induced ionization and molecular fragmentation are carried out. As a figure of merit, we calculate ion yields and the average charge state measured in recent experiments at the LCLS. We use a series of phenomenological models of increasing sophistication to unravel the mechanisms of the interaction of x rays with N_2 : a single atom, a symmetric-sharing model, and a fragmentation-matrix model are developed. The role of the formation and decay of single and double core holes, the metastable states of N_2^{2+} , and molecular fragmentation are explained.

PACS numbers: 33.80.-b, 33.80.Eh, 32.80.Aa, 41.60.Cr

I. INTRODUCTION

The theory of the interaction of ultrashort and intense x rays with atoms and molecules has recently come into focus by the newly-built x-ray free electron laser (FEL) Linac Coherent Light Source (LCLS) in Menlo Park, California, USA.^{1,2} The first experiments clearly revealed how important a detailed understanding of the interaction of x rays with single atoms and small molecules is for their interpretation.³⁻¹⁰ To obtain a clear theoretical view on the physics of the interaction with such comparatively simple systems represents a crucial piece of basic research; it is essential to form a foundation for studying

the interaction of more complex systems like condensed matter or biomolecules with intense x rays. Due to the novelty of x-ray FELs, there is currently little information available. Naively, one may suspect that the impact of x rays on matter depends only on the absorbed dose, i.e., the energy deposited per unit mass of medium. This would mean that the detailed pulse characteristics, i.e., duration, spatial profile, and temporal shape, are irrelevant. However, first theoretical and experimental studies of neon atoms give a lucid explanation why this is too simple a picture.^{3,9,11} In this work, we report on the theoretical foundation of the interaction of intense x rays with small molecules and particularly emphasize the additional challenges one faces over describing interactions with single atoms due to molecular fragmentation.

^{a)}Corresponding author; Electronic mail: christian.buth@web.de

One of the simplest molecules, nitrogen (N_2), was stud-

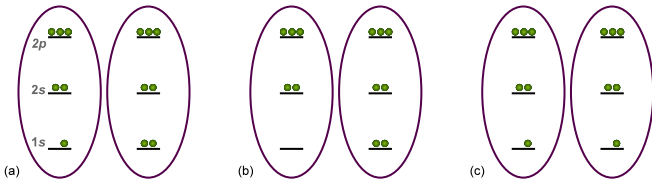


FIG. 1. (Color online) Classification of key types of core holes in N₂ in the localized core hole picture:^{12,13} (a) a singly-occupied spatial core orbital on one of the atoms of N₂: a single core hole (SCH), (b) a fully-depleted spatial core orbital on one N atom: a double core hole (DCH) on a single site (ssDCH), and (c) a singly-occupied spatial core orbital on both N atoms: a DCH on two sites (tsDCH).

ied extensively in the first experiments at LCLS^{4–8,10} and the multiphoton nature of the interaction was characterized. Specifically, Hoener *et al.*⁴ examined the interaction of x-ray pulses of constant energy but with varying duration and found in the ion yields the effect of frustrated x-ray absorption. Next, Fang *et al.*⁶ investigated the formation of (multiple) core holes; the most important core-hole types were found to be single core holes (SCHs), double core holes (DCHs) on a single site (ssDCH) and on two sites (tsDCH);^{12,13} all of them are depicted in Fig. 1. The tsDCH is a novel type of DCH which can be produced at third-generation synchrotrons only with very low probability;¹⁴ its abundant production has only become feasible with the emerging x-ray FELs.^{5,6,10,15} Further, Cryan *et al.*^{5,10} investigated the formation and decay of DCHs in laser aligned N₂ and the energy shift of DCHs with respect to the main SCH line where the synchronization between the optical laser and LCLS was achieved with the method of Glowia *et al.*;⁷ they found a clear sign of a nonspherical angular distribution of the Auger electrons in the molecular reference frame. Specifically, the experiments of Fang *et al.* and Cryan *et al.* open up novel perspectives for chemical analysis.^{12,13,15,16} Finally, Hau-Riege *et al.*⁸ investigated near-ultraviolet luminescence of N₂.

The prototypical N₂ molecule has also been studied extensively with other x-ray/XUV sources. Low-flux x rays from third-generation synchrotrons have been used to study the inner-shell properties of N₂^{17,18} and the dissociative one-x-ray-photon absorption cross section was measured.¹⁷ The production of SCHs by x-ray absorption results in Auger electron spectra from SCH decay that were classified in Refs. 19–23. For photon energies below the SCH-formation threshold, we note recent investigations at the Free Electron Laser in Hamburg (FLASH).^{24,25} The study of intense XUV absorption by N₂ at FLASH has a different character from x-ray absorption by N₂ at LCLS as the former radiation primarily targets valence electrons whereas the latter almost exclusively interacts with core electrons.

In contrast to the one-photon physics at present synchrotrons, the interaction of the x rays from FELs with

molecules is nonlinear. Namely, for intense x rays, several one-photon absorption events are linked by the decay widths of the created holes. So not only two or more photons are absorbed but the result of the absorption also depends on the time-difference between the individual one-photon absorption events. If it did not depend on the time-difference, the outcome of multiphoton absorption would only depend on the number of absorbed photons and not on the timing of the processes, i.e., the processes needed not be considered as an entity; however, due to the finite lifetime of inner-shell holes, the two events are linked and cannot be treated separately.

In this paper, we analyze theoretically the interaction of intense x rays with N₂. They represent the next step from studying the impact of x rays on single atoms like neon.^{3,9,11} Molecules in intense x-ray FEL light of high enough photon energy can be multiply core-ionized by sequentially absorbing several x-ray photons. Direct valence ionization occurs only rarely because the associated cross sections are orders of magnitude smaller than cross sections of core electrons.^{26–28} In very intense x rays, this may even lead to a hollowing out of molecules, i.e., core shells may be completely depleted due to ssDCH formation. For depleted shells, further ionization is drastically reduced and can even lead to transparency for x rays.²⁹ Significant ionization of hollowed out molecules resumes only when Auger decay refills the core shells. We will theoretically analyze the copiousness and influence of core holes for N₂ in intense x rays. We set out with an investigation of isolated N atoms and compute ion yields and the average charge state. Then, we consider N₂ molecules for which we have another possibility that has significant impact on observables; namely, as long as the molecular ion can be regarded as an entity, i.e., dissociation has not yet separated the molecule into fragments, the valence electrons are shared by both N atoms. This leads to a substantial redistribution of charge in decay processes of core-ionized molecules^{17,19–23} which has a significant influence on the observed ion yields from N₂ (and many other) quantities. Dicationic states N₂²⁺ are predominantly populated by Auger decay of SCHs; they are frequently metastable with respect to dissociation with comparatively long lifetimes.^{23,30} In this case, dissociation on a rapid timescale only resumes when more electrons are removed from the dication. This interdependence of multiple x-ray absorption and nuclear dynamics—which eventually leads to molecular fragmentation—poses a challenge to theoretical molecular physics. In the present study, we use a series of phenomenological models to unravel the complicated electronic and nuclear processes; it complements the phenomenological molecular rate-equation model³¹ described in Ref. 4.

The paper is structured as follows: we present a theoretical study of the absorption by N₂ of ultrashort and intense x-ray pulses from LCLS at a wavelength of 1.1 nm (1100 eV photon energy) with a nominal pulse energy of 0.15 mJ for FWHM pulse durations of 4 fs and a pulse

energy of 0.26 mJ for FWHM pulse durations of 7, 80, and 280 fs. For multiply-ionized N atoms, we use *ab initio* computations to determine Auger and fluorescence decay widths and the corresponding transition energies, electron binding energies, and one-x-ray-photon absorption cross sections [Sec. II]. We formulate a rate-equation model for an N atom and study the sequential absorption of multiple x-ray photons in Sec. III. Ion yields of a single N atom are predicted and show a strong deviation from the experimentally measured ion yields of N₂. The atomic rate-equations are, therefore, extended phenomenologically in Sec. IV to treat molecular fragmentation which is the cause for the observed differences between the ion yields of atoms and of molecules. For this purpose, a series of models of increasing sophistication is developed. In Sec. V, we explain the phenomenology of N₂ in intense x rays in terms of elemental molecular processes. Conclusions are drawn in Sec. VI.

Our equations are formulated in atomic units.³² For the conversion of a decay width Γ in electronvolts to a lifetime τ in femtoseconds, we use the relation $\tau = \frac{\hbar}{\Gamma} = \frac{0.658212 \text{ eV fs}}{\Gamma}$. All details of the models and calculations of this paper are provided in the supplementary materials.²⁸

II. ENERGIES AND DECAY WIDTHS OF MULTIPLY-IONIZED NITROGEN ATOMS

In this section, we study the energy levels of multiply-ionized N atoms and their decay widths and transition energies of Auger and radiative decay channels. They will be used to describe the interaction of atoms with x rays in rate-equation approximation in Sec. III. From the energy levels of multiply-charged N atoms, we identify the energetically accessible ionization channels for a specific x-ray photon energy because only those electrons are available for direct one-x-ray-photon ionization that have a lower binding energy than the photon energy. The transition energies for Auger decay and x-ray fluorescence allow an identification of the relevant processes in experimental electron and photon spectra. For elements from the second row of the periodic table, like nitrogen, only Auger decay is important, if a competing Auger decay channel exists in addition to x-ray fluorescence [Tables IV, VI and IX, XI in Ref. 28].

Energy levels, transition energies, and decay widths for multiply-ionized N atoms are calculated using the Dirac-Hartree-Slater (DHS) method.^{33,34} In the energy calculations, we use the DHS wave functions from the appropriate defect configurations to compute the expectation values of the total Hamiltonian including the Breit interaction,³³ i.e., a first-order correction to the local approximation is made. We also include the effects of relaxation by performing separate self-consistent field (SCF) calculations for the initial and final states [Δ SCF method] and take the difference of the total energies to obtain binding energies^{33,35} or transition energies, respectively. We calculate Auger and radiative decay widths with pertur-

bation theory^{34,36} from frozen-orbital and active-electron approximations as opposed to the relaxed-orbital calculations used to determine energies. The Auger matrix elements are calculated with DHS wave functions for the initial state with a proper defect configuration. Continuum wave functions are obtained by solving the Dirac-Slater equations with the same atomic potential as for the initial state. With this treatment, the orthogonality of the wave functions is assured. The radiative decay widths are calculated in multipole expansion using the relativistic length gauge for the electric multipoles.³⁶ The radial matrix elements are also calculated using DHS wave functions from the initial state. The effects of relaxation on the total *K*-shell Auger and radiative decay widths are less than 10 % for atoms with a *K*-shell vacancy.³⁷ For a few times ionized N atoms, the effects are even smaller of the order of only a few percent.

The relativistic calculations of energies and decay widths for a N atom yield values in the *jj* coupling scheme, i.e., they are specified with respect to electronic configurations which are labeled by $1s^\ell 2s^m 2p_{1/2}^{n_{1/2}} 2p_{3/2}^{n_{3/2}}$. Here, $0 \leq \ell, m, n_{1/2} \leq 2$, and $0 \leq n_{3/2} \leq 3$ are the occupation numbers of the respective orbitals where the subscripts 1/2 and 3/2 denote the value of the total angular momentum quantum number *j*.³⁸ By basing our method on DHS wave functions, we develop a more general approach than previous investigations, e.g., Ref. 39, by treating the atomic electronic structure in one-electron approximation including relativistic effects. The DHS approach yields good accuracy throughout the periodic table and facilitates to assess, and if necessary incorporate, such effects. For light elements like nitrogen, relativistic effects are small and have only minor importance for our modeling. Specifically, spin-orbit coupling is small which allows us to determine energies and decay widths in *LS* coupling—where the electronic configurations are denoted by $1s^\ell 2s^m 2p^n$ with $n = n_{1/2} + n_{3/2}$ —from the corresponding quantities in *jj* coupling scheme. Scalar relativistic effects are, nonetheless, accounted for in this procedure.

In the supplementary materials,²⁸ we discuss details of the probabilistic averaging of energies and decay widths in the *jj* coupling scheme and we provide following data for a multiply-ionized nitrogen atom: the electron binding energies are gathered in Tables III, VIII, and XIII; we list the Auger decay widths in Tables IV and IX with the corresponding transition energies provided in Tables V and X; the x-ray fluorescence decay widths are presented in Tables I, VI, and XI with the respective transition energies collected in Tables II, VII, and XII. Our Auger decay widths for SCHs in Table IV are in reasonable agreement with the early computations³⁹ of Bhalla.⁴⁰

III. ION YIELDS OF A NITROGEN ATOM

To describe the time-evolution of the absorption of x rays and the induced decay processes by a single

N atom, we use rate equations. This approach has proven useful in many problems of light-matter interaction and also for the interaction of x rays from free electron lasers with atoms.^{11,41–43} The justifications for this approximation are, first, that the envelope of the x-ray pulse varies slowly with respect to the change of populations of states, i.e., ionization and decay processes happen almost instantaneously on this time scale and, second, coherence effects are small; the x rays induce essentially only one-photon absorption processes which are, however, linked by inner-shell hole lifetimes.

The rate equations for a single nitrogen atom²⁸ comprise only electron removal terms and no electron addition terms because only the former are relevant for our study and the considered nitrogen charge states are always neutral or cationic. We include all possible one-x-ray-photon absorption processes in the independent electron approximation; the cross sections are obtained in one-electron approximation with the *Los Alamos National Laboratory Atomic Physics Codes*.^{44,45} All Auger decay widths of Sec. II are used, however, x-ray fluorescence is only accounted for when there is no competing Auger channel because Auger widths are typically orders of magnitude larger than the corresponding fluorescence widths.²⁸ Other contributions are neglected, specifically, cross sections for the simultaneous absorption of two x rays are tiny.⁹ Likewise more complicated and less important processes like shake off⁹ and double Auger decay⁴⁶ are not incorporated.

The probability to find an N atom at time t in an electronic configuration $1s^\ell 2s^m 2p^n$ is denoted by $P_{\ell mn}(t)$ where $\ell = m = 2$, $n = 3$ stands for the neutral atom. The x-ray photon flux at time t is given by $J_X(t)$, i.e., the number of x-ray photons that pass a unit area perpendicular to the beam in unit time.²⁶ The cross section at a chosen x-ray photon energy for the ionization of an electron of an N atom with electronic configuration $1s^\ell 2s^m 2p^n$ is denoted as $\sigma_{\ell mn}$ with $0 \leq \ell, m \leq 2 \wedge 0 \leq n \leq 3$. With these quantities, we formulate the rate equation to describe the depletion of the ground state of nitrogen due to x-ray absorption:

$$\frac{dP_{223}(t)}{dt} = -\sigma_{223} P_{223}(t) J_X(t). \quad (1)$$

The total (Auger plus x-ray fluorescence) decay width of a singly core-ionized state $1s^1 2s^2 2p^3$ is specified as Γ_{123} . The $1s$ ionization cross section of an N atom is denoted by $\sigma_{123 \leftarrow 223}$. Using these parameters, we find for the single core-hole rate

$$\frac{dP_{123}(t)}{dt} = (\sigma_{123 \leftarrow 223} P_{223}(t) - \sigma_{123} P_{123}(t)) J_X(t) - \Gamma_{123} P_{123}(t), \quad (2)$$

and analogously for the double core-hole rate

$$\frac{dP_{023}(t)}{dt} = (\sigma_{023 \leftarrow 123} P_{123}(t) - \sigma_{023} P_{023}(t)) J_X(t) - \Gamma_{023} P_{023}(t). \quad (3)$$

The three rate equations (1), (2), and (3) already are sufficient to describe the formation of SCHs and DCHs in an N atom. They form a system of ordinary linear differential equations which is solved numerically with *Mathematica*⁴⁷ for the following initial conditions: before the x-ray pulse, the N atom is in its electronic ground state, i.e., $P_{223}(-\infty) = 1$, and all other charge states are unpopulated, i.e., $P_{\ell mn}(-\infty) = 0$ for $\neg(\ell = m = 2 \wedge n = 3)$. Many more rate equations—36 in total—are needed to describe the ionization and various decay channels for all charge states from a neutral to a septuply-ionized N atom.

With the rate-equation description at hand, we can compute observables. The probability to find an initially neutral N atom in a cationic state with charge $0 \leq j \leq 7$ after the x-ray pulse is over ($t \rightarrow \infty$) is

$$P_j = \sum_{\substack{\ell+m+n=7-j \\ 0 \leq \ell, m \leq 2 \wedge 0 \leq n \leq 3}} P_{\ell mn}(\infty). \quad (4)$$

We define atomic ion yields to be normalized charge-state probabilities with $1 \leq j \leq 7$ by

$$Y_j = \frac{P_j}{1 - P_0}, \quad (5)$$

where $1 - P_0 = \sum_{k=1}^7 P_k$ is the probability to create a cation.

They are experimentally accessible and are a meeting point with theory.^{3,4} The Y_j can be used to determine an average charge state \bar{q} via

$$\bar{q} = \sum_{j=1}^7 j Y_j. \quad (6)$$

It is a useful gross quantity to characterize the x-ray induced ionization and quantifies the average amount of radiation damage caused.⁴

Exemplary charge-state probabilities (4) for an isolated N atom irradiated with intense x rays are shown in Fig. 2a for a range of photon energies from 0 to 2000 eV.²⁸ At low photon energies, certain ionization channels and, therefore, higher charge states are not accessible because the photon energy is not large enough to ionize inner electronic shells. Specifically, energies of shells move to higher binding energies with increasing charge state of the ions such that they move out of reach for a one-photon ionization process with fixed x-ray photon energy.¹¹ This is particularly clearly discernible in the range from 400 to 700 eV where steps indicate openings of ionization channels. Above 1200 eV, higher charge states decrease monotonically and the ground-state remains more and more populated because the cross sections have dropped substantially in magnitude such that the x rays do not ionize as effectively as before anymore.

The average charge state \bar{q} [Eq. (6)] for a single N atom in intense x rays is plotted in Fig. 2b for the same range of photon energies as in Fig. 2a. The above behavior of the

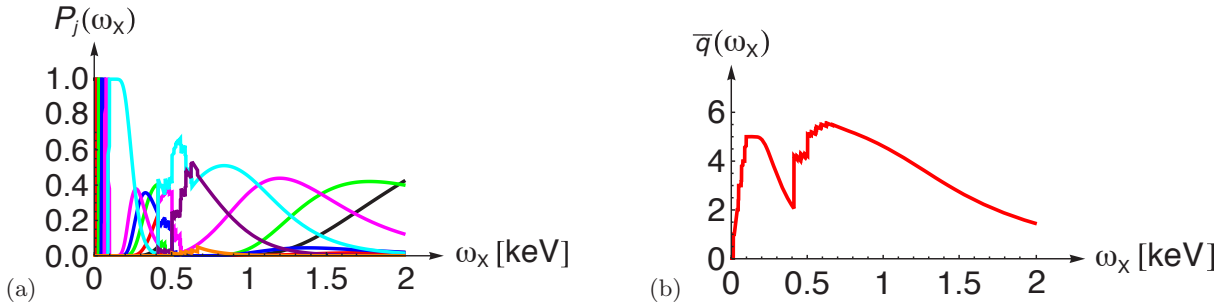


FIG. 2. (Color) An N atom after irradiation by x rays of constant spatial beam profile with a photon fluence (photon flux integrated over all times) of $8 \times 10^{11} \mu\text{m}^{-2}$ and a Gaussian temporal shape (7) with FWHM duration of 2 fs at varying photon energy ω_X . (a) Probabilities $P_j(\omega_X)$ from Eq. (4) to find an N atom in specific charge states: neutral (**black**), singly (**red**), doubly (**green**), triply (**blue**), quadruply (**magenta**), quintuply (**cyan**), sextuply (**purple**), and septuply (**orange**). (b) Average charge state $\bar{q}(\omega_X)$ from Eq. (6).

charge-state probabilities (4) is mirrored in the dependence of \bar{q} on the x-ray photon energy. For low photon energies, \bar{q} rises quickly due to large cross sections but its maximum value is limited by the energetic accessibility of electronic shells; it peaks, first, around 100 eV when the valence shells of N atoms can be fully depleted (Table III in Ref. 28) producing quintuply ionized final states and thus $\bar{q} = 5$. For higher photon energies \bar{q} drops again due to decreasing cross sections. Starting at about 400 eV also core electrons of nitrogen can be accessed leading to a second peak at about 700 eV when all electrons can be ionized. This peak does not reach the maximum value of $\bar{q} = 7$ because the x-ray fluence is too low to fully strip an N atom of its electrons. This is in contrast to the first peak where the maximum value is actually reached. Above 700 eV photon energy, \bar{q} drops monotonically due to decreasing cross sections.

To describe the interaction of finite pulses of limited transversal extend—along the x and y coordinates with respect to the propagation direction along the z axis—with an ensemble of atoms, we need to integrate over the temporal and spatial profiles of the incident x-ray pulse in the focal region. The LCLS is a FEL which operates by the self-amplification of spontaneous emission (SASE) principle^{48–50} which produces chaotic radiation pulses with random spikes. In principle, the pulse structure of SASE pulses needs to be taken into account in nonlinear optical processes. However, as exemplified for atoms in Ref. 11, the impact of chaotic light on linked one-photon processes—which are the predominant mode of interaction of intense x rays with nitrogen—has little impact. Therefore, there is no need to treat the explicit form of SASE pulses in this problem [see also Table II for a comparison of results for a Gaussian pulse with results from SASE pulses]. Instead, it is sufficient to use a Gaussian temporal profile for the rate of photons

$$\Gamma_X(t) = \Gamma_{X,0} e^{-4 \ln 2 \left(\frac{t}{\tau_X}\right)^2}, \quad (7)$$

with a peak rate of $\Gamma_{X,0} = 2 \sqrt{\frac{\ln 2}{\pi}} \frac{n_{\text{ph}}}{\tau_X}$ for n_{ph} photons

in the pulse and a full width at half maximum (FWHM) duration of τ_X . The number of photons n_{ph} is linked to the total energy in the pulse E_P via $n_{\text{ph}} = \frac{E_P}{\omega_X}$ for approximately monochromatic x rays with photon energy ω_X . The LCLS beam is modeled as a Gaussian beam⁴³ with a long Rayleigh range which implies that the spatial profile of the beam along its axis, the z axis, does not vary appreciably over the acceptance volume of the ion spectrometers. Therefore, the x-ray flux is approximately constant along the z axis and thus we may disregard its z dependence in what follows. There is, however, a substantial variation of the x-ray flux transversally to the beam axis. The transversal spatial profile of LCLS pulses was derived from ablation of solids in the FEL beam^{4,51–54} that yielded an elliptic profile with a FWHM length of the major and minor axes of $\varrho_x = 2.2 \mu\text{m}$ by $\varrho_y = 1.2 \mu\text{m}$, respectively. We have the following analytic expression for the transverse beam profile

$$\varrho(x, y) = \frac{4 \ln 2}{\pi \varrho_x \varrho_y} e^{-4 \ln 2 [(x/\varrho_x)^2 + (y/\varrho_y)^2]}; \quad (8)$$

it is normalized to unity with respect to an integration over the entire x - y plane, i.e., $\int_{-\infty}^{\infty} \int_{-\infty}^{\infty} \varrho(x, y) dx dy = 1$.

In our computations we find that an integration in the x - y plane over an area of $10^2 \mu\text{m}^2$ centered on the beam axis yields converged ratios of DCHs versus SCHs. Finally, the position-dependent x-ray flux follows from Eqs. (7) and (8) to

$$J'_X(x, y, t) = \varrho(x, y) \Gamma_X(t). \quad (9)$$

We use only a fraction of the nominal pulse energy^{3,4} to determine n_{ph} to account for losses in the experimental setup. This percentage is determined in Sec. IV B by a fit of experimental data with our theoretical predictions.

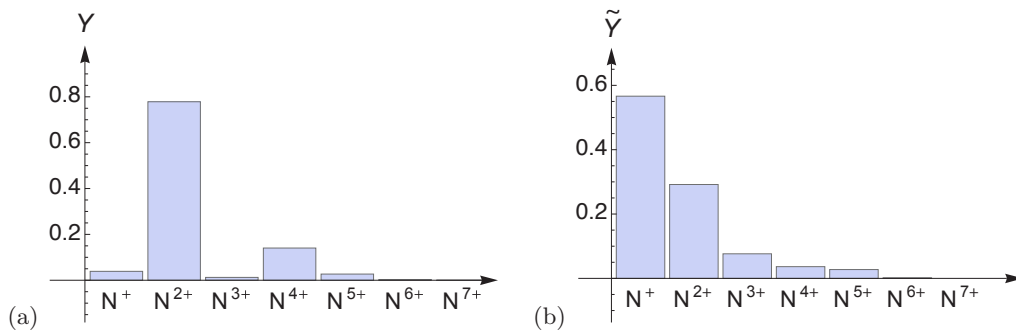


FIG. 3. (Color online) Ion yields of (a) an N atom and (b) an N₂ molecule irradiated by x rays of a FWHM duration of 280 fs and a photon energy of 1100 eV. In (a) we show theoretical results from the single atom model of Sec. III for the x-ray flux (9). We assume that only 31% of the nominal pulse energy of 0.26 mJ are actually available in the LCLS experiment [Table I]. In (b) we show experimental data for an N₂ molecule. The comparison of atomic Y_j with molecular \tilde{Y}_j ion yields for nitrogen clearly demonstrates the impact of molecular processes during and after the interaction with the x rays.

IV. ION YIELDS OF A NITROGEN MOLECULE

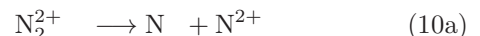
In the previous Sec. III, we discussed the ion yields of an isolated N atom which we denoted by Y_j for the positive charge $j \in \{1, \dots, 7\}$. In this section ion yields from an N₂ molecule—after fragmentation into atomic ions—are calculated to which we reference by \tilde{Y}_j . Figure 3 shows the theoretical ion yields for an N atom alongside the experimental data for an N₂ molecule; we find a stark difference between both bar charts. The trend found in the ion yields for a specific set of parameters solidifies, if we vary the pulse duration [Fig. 4] where we use \bar{q} [Eq. (6)] as a figure of merit.

At first sight, one may assume that the absorbed dose³ and thus the ionization of a sample of N₂ is very similar when the x-ray pulses have the same total energy and central wavelength and only one-photon absorption processes are included in the rate equations [Sec. IV]. If there was only a single one-photon process with cross section σ_1 , then the probability of ionization after the x-ray pulse would only depend on the x-ray fluence, i.e., $\sigma_1 \int_{-\infty}^{\infty} J_X(t) dt$, and thus be obviously independent of the time evolution of the x-ray flux $J_X(t)$. In Fig. 4, we display \bar{q} with respect to the x-ray pulse duration determined from the experimental data and for an N atom. One may expect naively that the absorbed dose is similar in all cases and \bar{q} is the same for all pulse durations, i.e., a horizontal line in Fig. 4. However, the contrary is true; we find a substantial dependence of \bar{q} on the pulse duration. This finding is indicative of (nonlinear) multi-x-ray-photon physics in the sample, i.e., the absorption of several x rays.

As expected from Fig. 3, there is a large discrepancy between \bar{q} for an N atom and the experimentally observed \bar{q} for N₂. These differences *cannot* be ascribed to molecular effects on photoionization cross sections⁵⁵ because they are small for the chosen photon energies which

are high above the ionization thresholds of multiply-charged N₂.^{18,55–57} Likewise fluorescence and Auger decay widths in molecules are usually well-represented by the respective values of the isolated atoms.

The differences between the molecular ion yields and the atomic ion yields in Fig. 3 are caused by the interplay of core ionization of N₂ with Auger decay, and nuclear dynamics. Namely, x-ray absorption by N₂ predominantly leads to SCH formation and N₂⁺ cations; unless more x rays are absorbed shortly after, the SCH Auger decays producing the molecular dication N₂²⁺. The N₂²⁺ fragments as follows:



where the probabilities for the channels (10a) and (10b) are 0.26 and 0.74, respectively.⁵⁸ The N₂²⁺ are an extreme case in the sense that the impact of molecular fragmentation is very pronounced on the ratio of N⁺ yield versus N²⁺ yield. The existence of the two fragmentation channels (10) offers a lucid explanation for the observed differences in Fig. 3 between atomic and molecular ion yields. For low x-ray flux, essentially no further x rays are absorbed prior to the Auger decay of a SCH in an N atom, i.e., the initially neutral atom ends up as N²⁺. However, for Auger decay of a SCH in N₂, the two charges, may be shared between both atoms (10b). This fact explains the large amount of N²⁺ ion yield for the atom versus the large N⁺ ion yield for the molecule in Fig. 3. A similar argument explains also the different ratio of the ion yields of N³⁺ versus N⁴⁺; namely, in the case that x-ray absorption is fairly slow—such that Auger decay and fragmentation mostly occur before another x ray is absorbed—a second x ray is more likely absorbed by a N⁺ fragment than a N²⁺ fragment as the former are more abundant than the latter. A subsequent Auger decay produces then preferably N³⁺ instead of N⁴⁺.

Despite the seemingly clear view on the physical reasons behind the deviations between Y_j and \tilde{Y}_j in Fig. 3,

one should bear in mind that N_2^{2+} possesses metastable dicationic states with respect to dissociation. The lifetime of N_2^{2+} can extend even to a few microseconds²³ for the dissociation through tunneling into the $N^+ + N^+$ continuum. In a laser-dissociation experiment,³⁰ 80 fs and 120 fs for the $N^+ + N^+$ and $N + N^{2+}$ fragmentation channels, respectively, were measured which are on a comparable time scale with the LCLS pulse durations discussed here. Consequently, the impact of the metastable dicationic states is to slow down fragmentation with a time constant of ~ 100 fs. This assessment is also supported by the fact that less than 2% of the N^+ peak in the time-of-flight spectra were ascribed to undissociated N_2^{2+} in Ref. 4. For metastable states, dissociation on a rapid timescale may only resume when more electrons are removed from the dication. In the following Secs. IV A and IV B, we present several phenomenological models to account for molecular fragmentation.

A. Symmetric-sharing model

Here we develop the simplest model of breakup of N_2 after irradiation by x rays in which charges produced by x-ray absorption on both N atoms are shared equally upon molecular fragmentation for an even number of charges; for an odd number of charges, one of the fragments carries one excess charge with respect to the other fragment. This model aims to contrast the extreme view of the single-atom model for ion yields of N_2 from Sec. III in which *no* redistribution of charge over the atoms in a molecule is accounted for in the course of the fragmentation process. Symmetric sharing is suggested in our situation by the dissociation of N_2^{2+} [Eq. (10)], the analysis of the potential energy curves of N_2^{3+} which indicate a most probable dissociation into $N^+ + N^{2+}$,⁵⁹ and laser-dissociation experiments of N_2^{4+} for which symmetric sharing was found to be the most prominent fragmentation channel.^{60,61} As a redistribution of charge—that is produced treating the atoms independently—never increases the maximum charge found on the involved atoms, the single-atom ion yields of Sec. III lead to an upper limit of the average charge state \tilde{q} from N_2 . Here we investigate the other extreme position which is to assume that the electrons of a charged N_2 molecule are always shared equally between both N atoms upon fragmentation. In other words, the charge on the two atoms of N_2 is determined independently and then redistributed between the two N atoms.²⁸ Such an equal sharing of charges leads to the smallest amount of positive charge per atom and thus to the lowest \tilde{q} . Hence it represents a lower limit to the observed charge-state distribution.

The \tilde{q} from the symmetric-sharing model is displayed in Fig. 4. Interestingly, we find that the lower limit is approached quite closely by the experimental data for short x ray pulses. However, the slow progression of the lower limit of \tilde{q} with the pulse duration leads to a signif-

icant deviation for longer pulses. This indicates that, for short pulses, there is mostly equal sharing of the charges between the atoms in N_2 while there is a different mechanism at work for longer pulses. Of course, this is related to the fact that the importance of the various processes entering the atomic rate equations of Sec. III are weighted differently depending on the actual LCLS pulse parameters. As will be discussed in detail in Sec. V, the principal reasons for the observed deviations is that during the long x-ray pulses, Auger decay processes mostly occur prior absorbing more x rays and fragmentation may happen in between. However, for short pulses, the molecule charges up quickly and nuclear expansion and fragmentation are of little importance on the time scale of the shortest (4 fs) pulse. In this case, only after the pulse is over, there is sufficient time for the induced nuclear wavepacket to evolve leading to molecular breakup.

B. Fragmentation-matrix model

To account for fragmentation of N_2 in the course of the interaction with x rays in a more realistic way, we make the following heuristic ansatz. We use the probabilities from the atomic rate equations after the x-ray pulse is over to form probabilities to find N_2 in various charge states treating the two N atoms as independent. The fragmentation of the molecular ion is then assumed to be determined only by the charges on the two atoms in terms of fixed ratios independent of the timing of the interaction with the x rays. This approximation is motivated by realizing that the fragmentation of N_2^{2+} —for which we have the two channels of Eq. (10)—depends only on the amount of N_2^{2+} produced in the course of the interaction with the x-ray pulse. A fixed fragmentation constant then accounts for the redistribution of charges. Introducing constants for all relevant fragmentation patterns of N_2 in all possible charge states leads to a fragmentation matrix which transforms the molecular probabilities from the independent atom treatment into molecular probabilities that account for charge redistribution from which ion yields are determined that can be compared with experimental data. Using a fixed fragmentation pattern clearly implies that we assume that fragmentation always occurs in the same way for a given independent-atom molecular charge state after the x-ray pulse is over, i.e., we neglect all dependencies on the actually involved intermediate states which change for different x-ray pulse parameters and dissociation during the x-ray pulse and focus exclusively on the achieved final independent-atom molecular charge state.

For a mathematical formulation of the fragmentation-matrix model, we set out from the atomic probabilities to find an N atom in various charge states after the x-ray pulse is over P_j with $0 \leq j \leq 7$. They are readily obtained from the solution of the atomic rate equations of Sec. III via Eq. (4). Independent-atom molecular probabilities P'_{ij} of N_2 for finding charge state i on the left

N atom and charge state j on the right N atom follow then immediately from $P'_{ij} = P_i P_j = P'_{ji}$ for $0 \leq i, j \leq 7$; they are aggregated in the vector \vec{P}' . The fragmentation matrix is denoted by \mathbf{F} ; it transforms the \vec{P}' into molecular probabilities that account for charge redistribution \vec{P} via

$$\vec{P} = \mathbf{F} \vec{P}' . \quad (11)$$

The vector \vec{P} is formed by the molecular probabilities $\tilde{P}_{ij} = \tilde{P}_{ji}$ to find $\text{N}_2^{(i+j)+}$. *Nota bene*, Eq. (11) needs to be applied for a single x-ray intensity; volume averaging (8) is performed for the transformed result. The atomic probabilities P_j [Eq. (4)] are recovered from Eq. (11) by choosing $\mathbf{F} = \mathbf{1}$. Summing over one index of \tilde{P}_{ij} then yields

$$P_j = \sum_{i=0}^7 \tilde{P}_{ij} \quad (12)$$

because $\sum_{i=0}^7 P_i = 1$ holds. Relation (12) is a general property of any \vec{P} from a meaningful \mathbf{F} to find the probabilities P_j of atomic fragments after molecular breakup. For an arbitrary \mathbf{F} , we find by setting \vec{P}' in Eq. (11) to Cartesian unit vectors that the sum of the matrix elements in each column of \mathbf{F} is unity, i.e., the sum of the elements of a vector remains the same (unity for probabilities) upon transformation with \mathbf{F} .

To find a form of \mathbf{F} that introduces a redistribution of charge, we make the additional assumption that a molecular ion will dissociate into fragments with similar charge states. Specifically, we assume that a molecular ion with an even number of electrons predominantly fragments symmetrically and, for an odd number of electrons, it fragments such that only one excess charge is found on one of the two fragments. As discussed previously, the independent-atom view [Sec. III] and the symmetric-sharing view [Sec. IV A] are two extreme positions with the former representing the upper limit of the average charge state [Eq. (6)] and the latter being its lower limit. Hence a redistribution of charge between the independent-atom channel and the symmetric-sharing channel, with a certain amount of probability shifted from the former to the latter, is able to represent the impact on \bar{q} even if more fragmentation channels are present for a specific molecular charge state. In other words, we realize that only the coupling of P'_{ij} for $|i - j| \geq 2$ to more symmetric charges needs to be considered for our purposes and a fraction $0 \leq f_{\{i,j\}} \leq 1$ of the probability of the charge state $\{i, j\}$ goes over into $\{k, l\} = \{(i+j)/2, (i+j)/2\}$ for even $i+j$ and into $\{k, l\} = \{(i+j-1)/2, (i+j+1)/2\}$ for odd $i+j$.⁶² This kind of redistribution of probability can be introduced easily using a transformation matrix $\mathcal{F}_{\{i,j\}}$ which differs from the identity matrix by setting $(\mathcal{F}_{\{i,j\}})_{(i,j),(i,j)} = (\mathcal{F}_{\{i,j\}})_{(j,i),(j,i)} = 1 - f_{\{i,j\}}$ and

τ_X [fs]	E_P [mJ]	$f_{\{0,3\}}$	$f_{\{0,4\}}$	$f_{\{2,4\}}$	$f_{\{0,5\}}$	$f_{\{2,5\}}$	$f_{\{0,6\}}$
280	0.31×0.26	0	0.54	1	0	0	1
80	0.25×0.26	0	0.61	1	0.26	0.17	1
7	0.16×0.26	0	1	1	1	1	1
4	0.26×0.15	1	1	0.48	1	0	0.65

TABLE I. Fragmentation constants for the most probable channels for the four pulse durations. Here, $f_{\{0,2\}} = 0.74$ in all cases [Eq. (10)]. The LCLS FWHM pulse duration is τ_X [Eq. (7)], the LCLS photon energy is 1100 eV, and the actually available pulse energy in the LCLS experiment is E_P . A nominal pulse energy of 0.15 mJ is specified for 4 fs pulses and 0.26 mJ for the remaining three pulse durations.

$(\mathcal{F}_{\{i,j\}})_{(k,l),(i,j)} = (\mathcal{F}_{\{i,j\}})_{(l,k),(j,i)} = f_{\{i,j\}}$. The set of 21 molecular charge states $\{i, j\}$ for which $|i - j| \geq 2$ holds is

$$K = \{\{0, 2\}, \{0, 3\}, \{0, 4\}, \{0, 5\}, \{0, 6\}, \{0, 7\}, \\ \{1, 3\}, \{1, 4\}, \{1, 5\}, \{1, 6\}, \{1, 7\}, \{2, 4\}, \\ \{2, 5\}, \{2, 6\}, \{2, 7\}, \{3, 5\}, \{3, 6\}, \{3, 7\}, \\ \{4, 6\}, \{4, 7\}, \{5, 7\}\} .$$

For all $k \in K$, we find a \mathcal{F}_k from which we construct the fragmentation matrix via $\mathbf{F} = \prod_{k \in K} \mathcal{F}_k$. As \mathcal{F}_k and \mathcal{F}_l commute for all $k, l \in K$ and matrix multiplication is associative, \mathbf{F} does not depend on the sequence of multiplication of the \mathcal{F}_k . The set K [Eq. (13)] contains all necessary molecular charge states to redistribute charges as is done in the symmetric-sharing model of Sec. IV A. Consequently, the probabilities of Sec. IV A are recovered by choosing $f_k = 1$ for all $k \in K$ and using Eq. (12).

Having asserted us that the fragmentation-matrix model correctly integrates both the single-atom model and the symmetric-sharing model, we need to find a good approximation for the 21 parameters in \mathbf{F} . As insufficient theoretical information has been published on the fragmentation of highly-charged N_2 , we need to find the parameters with the help of experimental data. The quest for the right parameters is further hindered by the fact that the nominal pulse energies specified differ from the actually available energies.^{3,4} The discrepancy between the nominal and the actual value of the pulse energy at the sample in the experiment is caused by losses in the beam line transmission which are not particularly well determined. In Ref. 4, it is specified that only 15%–35% of the nominal pulse energy arrive at the sample. In order to determine the fragmentation constants, we fit the theoretical ion yields from the fragmentation-matrix model [Eq. (5)] to the experimental ion yields of N_2 by minimizing the modulus of the difference between the average charge states (6) with respect to the fragmentation constants at the four measured x-ray pulse durations, i.e., for 4, 7, 80, and 280 fs.²⁸ Thereby, we adjust the pulse energies such that the constant for the fragmentation of N_2^{2+} [Eq. (10)], $f_{\{0,2\}} = 0.74$, i.e., the experimen-

tal value for fragmentation after Auger decay of a SCH is recovered. This procedure yields the fragmentation constants and the fractions of the nominal pulse energy that are listed in Table I. Note that this approach assumes that the molecular charge state $\{0, 2\}$ is predominantly produced by SCH decay, i.e., the competing processes of double valence ionization by x rays is neglected because of tiny cross sections.

A number of insights about the experiment can be gained by inspecting Table I. Examining E_P , we find that the actually available pulse energy in the experiment is with one exception in the range 25–31% of the nominal pulse energy. Only the pulse energy for 7 fs pulses is around 16% of the nominal pulse energy of 0.26 mJ. This drop can be rationalized by taking 28% of 0.15 mJ—the nominal pulse energy specified for the case of 4 fs pulses—which leads to the same actual pulse energy as 16% of 0.26 mJ. The value 28% is consistent with the percentages of the other pulse durations and indicates that potentially there was a drop in the actual output of LCLS when going to so short pulses. The range 25–31% is higher than the value of $\sim 23\%$ specified in Ref. 3 for 1050 eV photon energy. The peak x-ray intensities follow to 3.1×10^{17} W/cm², 1.7×10^{17} W/cm², 2.6×10^{16} W/cm², and 9.0×10^{15} W/cm² for the nominal pulse durations 4, 7, 80, and 280 fs, respectively.

The change of molecular fragmentation with pulse parameters can be read off Table I. Predominantly, $f_{\{0,2\}}$ is determined by the absorption of one x ray, $f_{\{0,3\}}$ and $f_{\{0,4\}}$ are from two-x-ray-absorption, $f_{\{2,4\}}$, $f_{\{0,5\}}$, and $f_{\{0,6\}}$ are from three-x-ray-absorption, and $f_{\{2,5\}}$ is from four-x-ray-absorption. Apart from $f_{\{2,4\}}$ and $f_{\{0,6\}}$ the fragmentation constants overall increase with decreasing pulse duration. This indicates that symmetric sharing becomes very important for the shortest pulses while molecular fragmentation may occur during the longer pulse prior absorption of further x rays. Due to very low probabilities, the values for $f_{\{2,4\}}$, $f_{\{2,5\}}$, and $f_{\{0,6\}}$ for 4 fs pulses are not important. As $f_{\{2,4\}}$ and $f_{\{0,6\}}$ are basically unchanged for all pulse durations, the associated fragmentation process is ascribed to the core-hole lifetimes which are independent of the pulse duration.

The merits of the fragmentation matrix model are exhibited in Figs. 4 and 5 where we plot \tilde{q} and the ion yields, respectively, from the model alongside the experimental data. The agreement of our theoretical \tilde{q} with the experimental \tilde{q} is very good, however, despite fitting the fragmentation matrix at all points, the two \tilde{q} do not coincide. This has several reasons. First, the fit is not arbitrary but physically motivated by the molecular breakup process relying on the probabilities to find the atom in various charge states. The atomic rate equations of Sec. III were designed carefully, yet only a one-electron approximation has been used and particularly shake off is not treated.^{3,9} Other works on neon atoms^{3,9} show a far less than perfect agreement of atomic ion yields from experiment with theory. In the light of Refs. 3 and 9, our theoretical ion yields in Fig. 5 appear almost too close to

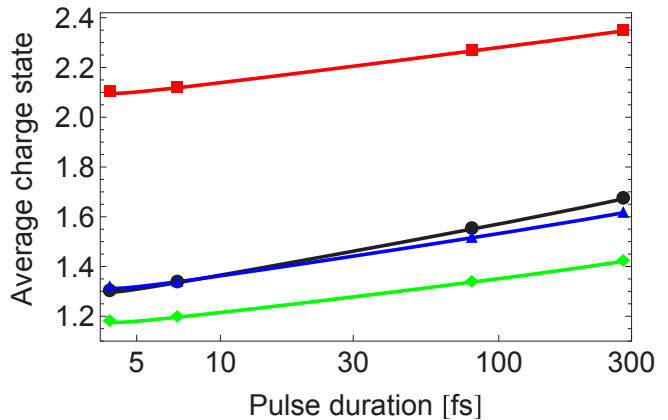


FIG. 4. (Color online) Average charge state \tilde{q} from N_2 subject to LCLS x-ray pulses of varying FWHM duration. We show \tilde{q} deduced from the experimental ion yields of N_2 [Fig. 5] for the nominal pulse durations 4, 7, 80, and 280 fs, alongside our calculations; the points are connected by interpolation. Specifically, we plot the experimental \tilde{q} as **black** circles, \tilde{q} from a single N atom as **red** squares [Sec. III], \tilde{q} from the symmetric-sharing model as **green** diamonds [Sec. IV A], and \tilde{q} from the fragmentation-matrix model [Sec. IV B] as **blue** triangles. See Table I for further LCLS pulse parameters.

the experimental ones.

The finding that \tilde{q} from the fragmentation-matrix model is lower than the experimental \tilde{q} for longer pulses is ascribed to the fact that no fragmentation during the pulse is treated. Namely, the fragmentation time of N_2^{2+} is³⁰ ~ 100 fs and thus shorter than the longest, 280 fs, LCLS pulses. Hence molecular fragmentation of N_2^{2+} may occur before the x-ray pulse is over. When N_2^{2+} fragments into $N^+ + N^+$, absorption of another x ray by the atomic ions N^+ leads to an enhancement of the N^{3+} yield; fragmentation into $N + N^{2+}$ increases the N^{2+} and N^{4+} yields. The fragmentation-matrix model does not distinguish this case from breakup of the respective molecular ions which cannot be treated by static ratios. A time- and molecular-state-dependent fragmentation matrix should be able to fully account for the observed molecular ion yields.

Finally, we used the nominal pulse duration in all calculations so far as was done in Ref. 4. However, the pulse duration was found to be significantly shorter in experiments.^{3,63} Namely, a nominal pulse duration of 80 fs was estimated actually to be 20–40 fs in Ref. 3 and measured to be 40 fs in Ref. 63; the nominal pulse duration of 300 fs pulses was found to be 120 fs.⁶³ Yet the experimental conditions in the two studies Refs. 3 and 63 differ somewhat from the one in Ref. 4. Fortunately, the dependence of our theoretical predictions on the pulse duration turns out to be quite low.²⁸

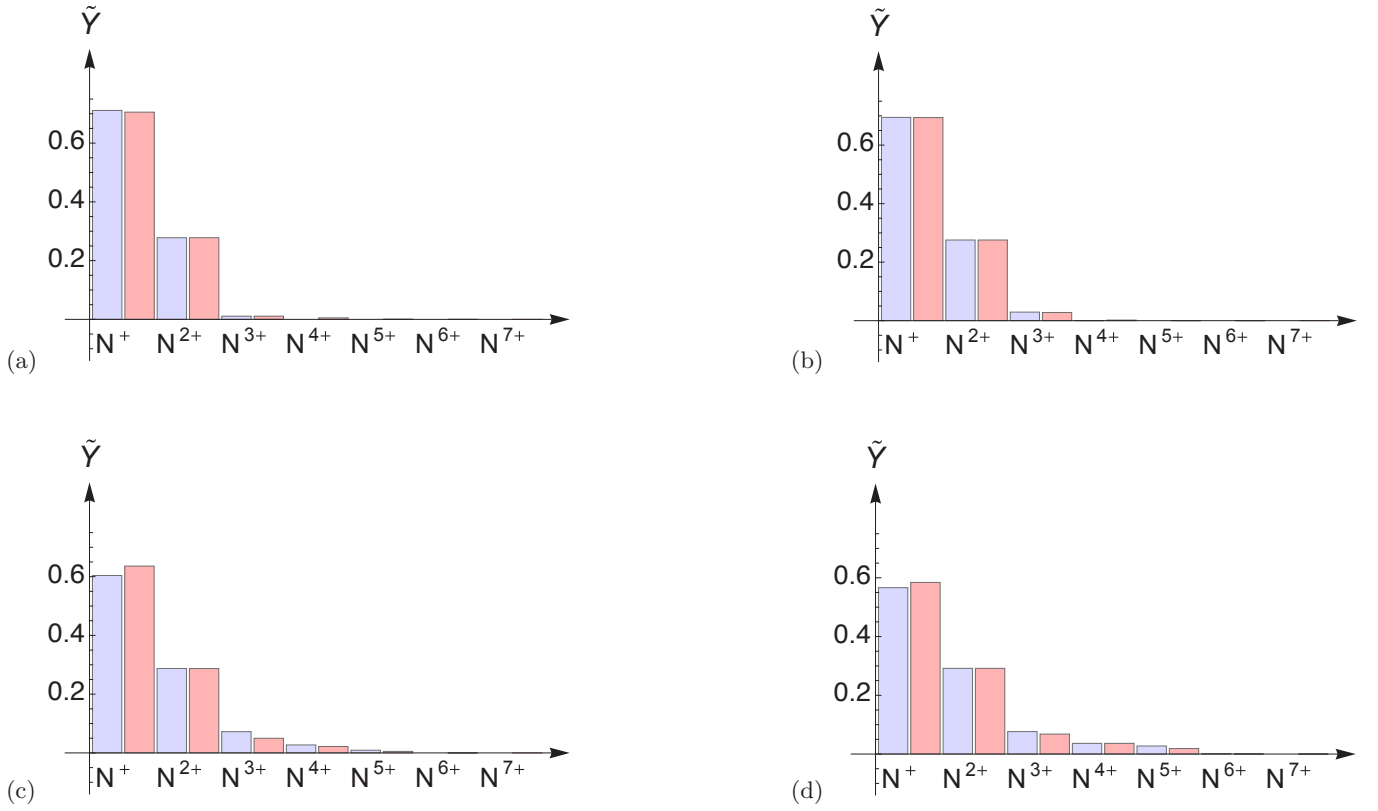


FIG. 5. (Color) Ion yields \tilde{Y}_j of N_2 subject to LCLS x-ray pulses of varying duration: (a) 4 fs, (b) 7 fs, (c) 80 fs, and (d) 280 fs. Experimental \tilde{Y}_j are given by the blue bars and theoretical \tilde{Y}_j from the fragmentation-matrix model [Sec. IV B] by the red bars. See Table I for further LCLS pulse parameters.

V. EXPLANATION OF THE OBSERVED PHENOMENA IN TERMS OF ELEMENTAL MOLECULAR PROCESSES

In the previous Secs. III, IV A, and IV B, we investigated phenomenological models that are based on the solution of the atomic rate equations to describe the interaction of N_2 with x rays where we used the average charge state \tilde{q} [Eq. (6)] as a figure of merit to assess the quality of our models. Here we discuss the problem from the perspective of the processes entering the atomic rate equations to unravel the elemental molecular processes that give rise to the behavior of the experimental \tilde{q} in Fig. 4. In Refs. 4 and 31, a molecular-rate-equation model has been discussed based on elemental molecular processes which differs in various aspects from the following analysis.

To describe the elemental molecular processes of N_2 in intense x rays, we need to find out, first, which molecular electronic configurations prevail in the course of the interaction with the x-ray pulse. As the atomic ionization cross sections for core electrons are orders of magnitude larger than cross sections for valence electrons, predominantly core electrons are ionized. The probabilities to find N_2 in its ground state or with a SCH, a

tsDCH, or a ssDCH can be deduced from the solution of the atomic rate equations for an N atom via $P_{223}(t)^2$, $2P_{123}(t)P_{223}(t)$, $P_{123}(t)P_{123}(t)$, and $P_{023}(t)P_{223}(t)$, respectively. Furthermore, a sequence of photoionization (P) with a following Auger decay (A) and another photoionization (PAP) is a competing process to DCHs for two-x-ray-photon absorption.^{11,28} These probabilities are shown in Fig. 6 for a short-pulse (4 fs) and a long-pulse (280 fs) scenario. It is revealed clearly that for the long pulse [Fig. 6b], we have a contribution from almost exclusively SCHs and PAPs with an almost vanishing probability to find DCHs. On the contrary, for the short pulse, PAPs are less important due to the fact that the Auger decay time of a SCH²⁸ of 6.7 fs is longer than the pulse duration. Therefore, DCHs are more relevant for the short pulse [Fig. 6a] where tsDCHs make a larger contribution than ssDCHs. This is due to the bigger cross sections for the formation of tsDCHs compared with ssDCHs and the longer lifetime of the former with respect to the latter. Namely, for an N atom in x-ray light at 1100 eV photon energy, the cross section for SCH formation is 56 kbarn and it is 34 kbarn for DCH formation. The SCH formation cross section is, therefore, by a factor of 1.7 higher than the cross section for DCH formation in an N atom but ssDCHs

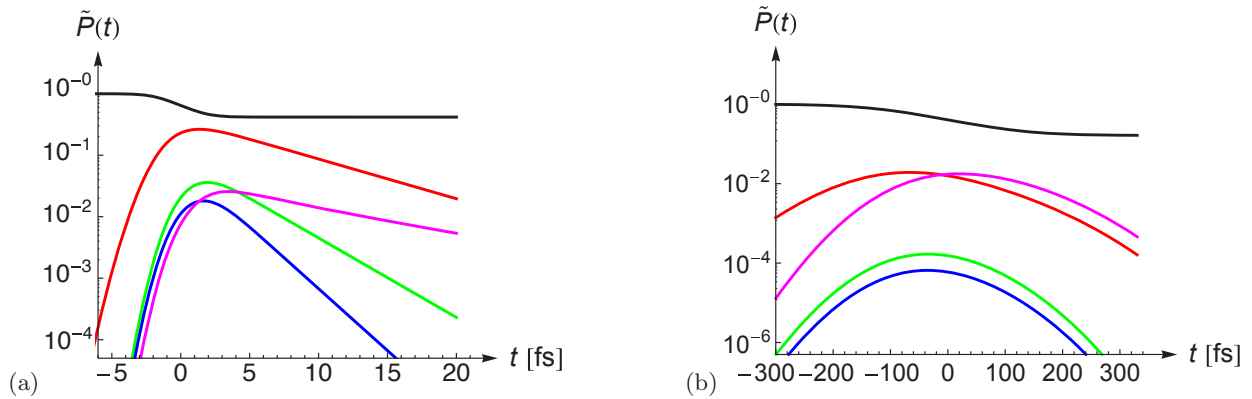


FIG. 6. (Color) The probabilities $\tilde{P}(t)$ to find N_2 during the x-ray pulse in its ground state is given by the **black** lines; the **red** lines are the probability for a SCH; the **green** and **blue** lines stand for the probability to find a tsDCH and a ssDCH, respectively; the PAPs are indicated by **magenta** lines. Probabilities are determined for (a) a Gaussian short pulse (7) of a FWHM duration of 4 fs and (b) a Gaussian long pulse of a FWHM duration of 280 fs. See Table I for further LCLS pulse parameters.

in N_2 , nevertheless, make a noticeable contribution for short pulses, i.e., higher x-ray intensities, as is revealed in Fig. 6a. The lifetime of a tsDCH is half the lifetime of a SCH, i.e., $6.7 \text{ fs}/2 = 3.4 \text{ fs}$, versus 2.2 fs for a ssDCH, respectively [Tables IV and IX of Ref. 28]. The conclusions drawn from Fig. 6 are corroborated by the ratios in Table II to find SCH decay, first decay of DCHs, and PAPs after volume integration (8). We also show the impact of the SASE pulse structure^{48–50} on the ratios using the partial coherence method to generate SASE pulses^{25,64,65} with 8 eV bandwidth and a Gaussian temporal envelope that has the same FWHM after squaring as the Gaussian pulse used to compute the reference ratios and make Fig. 6. Inspecting Table II, we find that the impact of the SASE pulse structure on the resulting ratios is small as has also been found in previous work.¹¹

Another reason why SCH, ssDCH, tsDCH, and PAP channels have a particular importance is the fact that N_2^+ and N_2^{2+} are metastable with respect to dissociation,^{23,30} i.e., the molecular ion remains essentially intact until it has charged up to N_2^{3+} and higher.⁵⁹ Therefore, these channels dominate the first stages of the interaction of N_2 with x rays and thus have a crucial impact on fragmentation products and such on molecular ion yields. Similarly, for very high intensities, also N_2 with triple and quadruple core holes may occur. However, for our parameters, Fig. 6 reveals that we need to focus only on a very limit number of initial molecular channels. Based on the discussion of Secs. III, IV A, and IV B, we deduce that one needs to consider following elemental molecular processes:

First, for long pulses with moderate x-ray photon flux, where the probability to absorb two x rays in a few-femtosecond time interval is low, N_2^{2+} frequently fragments into two atomic ions prior to absorbing further x rays. However, for a higher x-ray flux this probability is not low and differences may arise due to further ab-

sorption of x rays prior to molecular dissociation. This introduces a time scale of $\sim 100 \text{ fs}$ that determines the rate of fragmentation of the dication N_2^{2+} [Ref. 30].

Second, for high enough x-ray intensities, further photoionization and Auger decay of the molecular dication N_2^{2+} prior fragmentation forms molecular trications N_2^{3+} . No bound states were found for N_2^{3+} ions in the midst of many Coulomb repulsive potential surfaces.^{59,66} Therefore, one may assume that those N_2^{3+} without core holes fragment into N^{2+} and N^+ which is the channel that is indicated most prominently by the potential energy surfaces. There is only a small amount of N_2^{3+} produced without core holes in the present case due to small valence ionization cross sections for x rays. Although N_2^{3+} is not metastable, dissociation is not immediate and further x rays may be absorbed prior dissociation. Specifically, N_2^{3+} with core holes should still be considered as a molecular entity which is only broken up after Auger decay because of the faster time scale of Auger decay compared with molecular fragmentation.

Third, the sequence of two absorptions of an x rays with subsequent Auger decays (PAPAs) or, likewise, the two Auger decays of a DCH leads to N_2^{4+} . There is hardly any difference between the two situations concerning the way molecular fragmentation takes place. A SCH decay leads to N_2^{2+} which is metastable with a lifetime that is large compared with inner-shell hole lifetimes.^{23,28,30} The absorption of a second x ray then leads to N_2^{3+} which is *not* metastable^{59,66} and the molecular ion starts to dissociate, however, on a much slower time scale than Auger decay. The Auger decay time scale is independent of the x-ray pulse duration. As shown in Table II, PAPAs are comparable with the first decay of ssDCHs in the 4 fs case and PAPAs thus are an important channel for two-x-ray-photon absorption. Furthermore, only a DCH is metastable with respect to dissociation; as soon as the first Auger decay of a DCH occurs, N_2^{3+} is formed

τ_X [fs]	Pulse	SCH decay	ssDCH decay	tsDCH decay	PAPA
4	1 SASE	0.87	0.049	0.079	0.052
	10 SASE	0.88	0.046	0.073	0.045
	100 SASE	0.87	0.050	0.080	0.045
	1000 SASE	0.87	0.050	0.081	0.046
	Gaussian	0.89	0.041	0.065	0.035
280	1 SASE	0.99	0.0035	0.0058	0.28
	10 SASE	0.99	0.0045	0.0074	0.33
	100 SASE	0.99	0.0044	0.0072	0.33
	Gaussian	0.99	0.0043	0.0072	0.33

TABLE II. Ratios to find SCH decay, first tsDCHs decay, the first ssDCHs decay, and a PAPA process after averaging over a varying numbers of SASE pulses and from a Gaussian pulse with a FWHM duration of τ_X . The ratios are probabilities from volume averaging (8) which are renormalized to the sum of the probabilities for (the first) decay of SCHs, tsDCHs, and ssDCHs. See Table I for further LCLS pulse parameters.

which starts to dissociate in straight analogy to PAP after the absorption of the second x ray. The second Auger decay of a DCH is on the same time scale as for the PAPA process. As both processes describe very similar situations with respect to molecular fragmentation, they have the same fragmentation pattern. From our findings with the symmetric-sharing model [Sec. IV A] and results from laser-dissociation experiments,^{60,61} we may assume equal sharing of the four charges between the two nitrogen nuclei for the fragmentation of N_2^{4+} ions. This is corroborated by inspecting Fig. 5a where no significant ion yield for N^{3+} is found which would arise from a nonsymmetric sharing of charges for the fragmentation of N_2^{4+} ions resulting from DCHs or PAPAs. In our case, DCHs and PAPAs affect results for the short and long pulses where the importance of DCHs is larger for the high x-ray flux of short pulses because the molecules are ionized faster. Fragmentation predominantly occurs after the short pulses are over. For long pulses, the x-ray flux is reduced leading to a slower rate of photoabsorption and frequently fragmentation of N_2^{2+} occurs before further x rays are absorbed.

Fourth, for even higher charge states, dissociation becomes more and more rapid but the involved time scale needs, nonetheless, be considered. Namely, for x-ray pulses of only a few femtoseconds, dissociation does not play a substantial role and thus the assumptions underlying the fragmentation-matrix model [Sec. IV B] are well fulfilled. In this case, also for highly-charged N_2 , symmetric sharing should be the predominant mode of fragmentation.⁶⁶ For long x-ray pulses, breakup frequently occurs before high molecular charge states are reached and subsequent x-ray absorption occurs by independent ions.

The above analysis suggests that molecular effects and molecular fragmentation of N_2 in intense x rays are centered around these four steps. The described elemental molecular processes should characterize the most important aspects of the phenomenology of the interaction

as all insights gained from the analysis of the models of Secs. III, IV A, and IV B are incorporated.

VI. CONCLUSION

In this paper, we discuss theoretically the interaction of intense, short-pulse x rays from the novel x-ray free electron laser Linac Coherent Light Source (LCLS) with N_2 molecules. We set out from the computation of the energies, decay widths, and one-x-ray-photon absorption cross sections of a single N atom. These data are input to describe the interaction an N atom with x-ray pulses in terms of a rate-equation model. Ion yields and the average charge state are computed and compared with experimental data for N_2 . The agreement of theoretical data for an N atom and experimental data for N_2 is not satisfactory which we ascribe to a fragmentation of N_2 after ionization causing a redistribution of charges over both atoms in the molecule. To describe the molecular degrees of freedom, we devise two phenomenological models. First, we compute a lower limit to the average charge state assuming always equal sharing of charges between both atoms in N_2 . Second, we use a fragmentation matrix to treat molecular dissociation with static ratios to relate atomic and molecular ion yields. The models clearly indicates the relevance of the redistribution of charge and a different weighting of processes on short and long time scales for similar nominal x-ray pulse energy. The formation of high charge states at short pulse durations is suppressed by a redistribution of charge in the multiply-ionized molecule giving rise to the observed frustrated absorption.⁴

Pertinent to our atomic rate equations of Sec. III, however, is—as was shown by Young *et al.*³ for neon atoms—that the deviation of the theoretical ion yields from the experimental ones in the intense x rays of LCLS becomes more and more pronounced when the photon energy is of the order of 2000 eV. The reason of this deviation is the

fact that in Ref. 3, the rate equations for a neon atom contain only all possible one-photon absorption and fluorescence and Auger decay channels as is also the case for our rate-equation model of an N atom [Sec. III]. However, at such high photon energies, other channels involving many-electron effects like shake off (for neon atoms in Ref. 9) may become important. As in the present study of N₂, the photon energy of 1100 eV also is high above the SCH-ionization threshold of an N atom, a similar deviation, as was found for neon,^{3,9} may be relevant. However, we do not investigate this issue due to a lack of experimental data on single N atoms in intense x rays.

Although our theoretical analysis is centered on N₂, we believe that many of our conclusions are generally true. The time scale of the involved processes is dictated by the formation and decay of SCHs and DCHs. Higher numbers of core holes than one DCH per N₂ are of little importance at the present x-ray intensities. Molecular fragmentation depends largely on the pacing of x-ray absorption and, related, the abundance of SCHs versus DCHs. For x-ray irradiation durations of only a few femtoseconds, nuclear dynamics—specifically due to Coulomb explosion of the charged fragments—does not play a role during the x-ray pulse and we may assume fixed nuclei in the equilibrium geometry of the molecule. However, the nuclear wavepacket generated leads to a subsequent fragmentation of the molecule. Instead, for longer pulse durations, nuclear expansion during the x-ray pulse becomes a crucial issue. A molecule with a SCH may be metastable with respect to dissociation and may even remain metastable after Auger decay has taken place. Clearly, this is crucial for the understanding of the observed ion yields. Hence molecular effects and molecular fragmentation are centered around these initial steps. For a general description of molecules in intense x rays, one needs to account for the complicated joint problem of x-ray absorption, decay processes, and nuclear dynamics. We make first attempts towards a full treatment of the problem.

Based on our studies, many fascinating possibilities for future research open up. An investigation with *ab initio* methods of molecular physics³² of the absorption of x rays, the decay of inner-shell holes and the resulting nuclear dynamics poses a challenge. Nonetheless, we consider it of high importance to find an *ab initio* description to gain deeper insights and to establish a theoretical foundation for molecules in intense x rays. The formation of DCHs gives one detailed information about the structure of a molecule; it was found to be more sensitive than SCH spectroscopy.^{12,13,15,16} The time-delay between the two core-hole ionization events in DCH production needs to be short enough, such that the first vacancy has not decayed. Then the second photoelectron carries detailed information about the dicationic states of the molecule. This gives rise to x-ray two-photon photoelectron spectroscopy (XTTPS).¹⁶ Furthermore, we have a valence electron density in molecules that may differ appreciably from the density produced by the noninteracting atoms

in the molecular geometry. This may in some cases have a noticeable influence on the rate of intraatomic electronic decay (IAED),⁶⁷ if valence electrons are involved. Additionally, the close packing of the atoms in a molecule gives rise to interatomic electronic decay processes for inner-valence holes, namely, interatomic Coulombic decay (ICD) and electron transfer mediated decay (ETMD) (Ref. 67 and References therein). The relevance of these additional channels needs to be assessed in future work.

ACKNOWLEDGMENTS

C.B. would like to thank Nikolai V. Kryzhevoi for fruitful discussions and a critical reading of the manuscript. We are grateful to Oleg Kornilov and Oliver Gessner for discussions on nitrogen molecules in intense x rays. C.B. was supported by the National Science Foundation under grant Nos. PHY-0701372 and PHY-0449235 and by a Marie Curie International Reintegration Grant within the 7th European Community Framework Program (call identifier: FP7-PEOPLE-2010-RG, proposal No. 266551). J.-C.L. thanks for support by the Fundamental Research Funds for the Central Universities. Additional funding was provided by the Office of Basic Energy Sciences, Office of Science, U.S. Department of Energy, for C.B. under Contract No. DE-AC02-06CH11357 and for L.F., M.H., and N.B. under Contract No. DE-FG02-92ER14299. M.H.C.'s work was performed under the auspices of the U.S. Department of Energy by Lawrence Livermore National Laboratory under Contract No. DE-AC52-07NA27344. R.N.C. is supported through the LCLS at the SLAC National Accelerator Laboratory by the U.S. Department of Energy, Office of Basic Energy Sciences. J.P.C. and J.M.G. are supported through both the LCLS and The PULSE Institute for Ultrafast Energy Science at the SLAC National Accelerator Laboratory by the U.S. Department of Energy, Office of Basic Energy Sciences. Portions of this research were carried out at the Linac Coherent Light Source (LCLS) at SLAC National Accelerator Laboratory. LCLS is an Office of Science User Facility operated for the U.S. Department of Energy Office of Science by Stanford University.

REFERENCES

- ¹J. Arthur, P. Anfinrud, P. Audebert, K. Bane, I. Ben-Zvi, V. Bharadwaj, R. Bionta, P. Bolton, M. Borland, P. H. Bucksbaum, R. C. Cauble, J. Clendenin, M. Cornacchia, G. Decker, P. Den Hartog, S. Dierker, D. Dowell, D. Dungan, P. Emma, I. Evans, G. Faigel, R. Falcone, W. M. Fawley, M. Ferrario, A. S. Fisher, R. R. Freeman, J. Frisch, J. Galayda, J.-C. Gauthier, S. Gierman, E. Gluskin, W. Graves, J. Hajdu, J. Hastings, K. Hodgson, Z. Huang, R. Humphry, P. Ilinski, D. Imre, C. Jacobsen, C.-C. Kao, K. R. Kase, K.-J.

- Kim, R. Kirby, J. Kirz, L. Klaisner, P. Krejcik, K. Kulan-
 der, O. L. Landen, R. W. Lee, C. Lewis, C. Lim-
 borg, E. I. Lindau, A. Lumpkin, G. Materlik, S. Mao,
 J. Miao, S. Mochrie, E. Moog, S. Milton, G. Mul-
 hollan, K. Nelson, W. R. Nelson, R. Neutze, A. Ng,
 D. Nguyen, H.-D. Nuhn, D. T. Palmer, J. M. Pater-
 son, C. Pellegrini, S. Reiche, M. Renner, D. Riley,
 C. V. Robinson, S. H. Rokni, S. J. Rose, J. Rosen-
 zweig, R. Ruland, G. Ruocco, D. Saenz, S. Sasaki,
 D. Sayre, J. Schmerge, D. Schneider, C. Schroeder,
 L. Serafini, F. Sette, S. Sinha, D. van der Spoel,
 B. Stephenson, G. Stupakov, M. Sutton, A. Szöke,
 R. Tatchyn, A. Toor, E. Trakhtenberg, I. Vasser-
 man, N. Vinokurov, X. J. Wang, D. Waltz, J. S.
 Wark, E. Weckert, Wilson-Squire Group, H. Winick,
 M. Woodley, A. Wootton, M. Wulff, M. Xie, R. Yotam,
 L. Young, and A. Zewail, *Linac coherent light source
 (LCLS): Conceptual design report*, SLAC-R-593, UC-
 414 (2002) www-ssrl.slac.stanford.edu/lcls/cdr.
- ²P. Emma, R. Akre, J. Arthur, R. Bionta, C. Bostedt,
 J. Bozek, A. Brachmann, P. Bucksbaum, R. Coffee, F.-
 J. Decker, Y. Ding, D. Dowell, S. Edstrom, J. Fisher,
 A. Frisch, S. Gilevich, J. Hastings, G. Hays, P. Her-
 ing, Z. Huang, R. Iverson, H. Loos, M. Messerschmidt,
 A. Miahnahri, S. Moeller, H.-D. Nuhn, G. Pile, D. Rat-
 ner, J. Rzepiela, D. Schultz, T. Smith, P. Stefan,
 H. Tompkins, J. Turner, J. Welch, W. White, J. Wu,
 G. Yocky, and J. Galayda, *Nature Photon.*, **4**, 641
 (2010).
- ³L. Young, E. P. Kanter, B. Krässig, Y. Li, A. M. March,
 S. T. Pratt, R. Santra, S. H. Southworth, N. Rohringer,
 L. F. DiMauro, G. Doumy, C. A. Roedig, N. Berrah,
 L. Fang, M. Hoener, P. H. Bucksbaum, J. P. Cryan,
 S. Ghimire, J. M. Glowonia, D. A. Reis, J. D. Bozek,
 C. Bostedt, and M. Messerschmidt, *Nature*, **466**, 56
 (2010).
- ⁴M. Hoener, L. Fang, O. Kornilov, O. Gessner, S. T.
 Pratt, M. Gühr, E. P. Kanter, C. Blaga, C. Bost-
 edt, J. D. Bozek, P. H. Bucksbaum, C. Buth,
 M. Chen, R. Coffee, J. Cryan, L. DiMauro, M. Glow-
 nia, E. Hosler, E. Kukk, S. R. Leone, B. McFarland,
 M. Messerschmidt, B. Murphy, V. Petrovic, D. Rolles,
 and N. Berrah, *Phys. Rev. Lett.*, **104**, 253002 (2010).
- ⁵J. P. Cryan, J. M. Glowonia, J. Andreasson, A. Belka-
 cem, N. Berrah, C. I. Blaga, C. Bostedt, J. Bozek,
 C. Buth, L. F. DiMauro, L. Fang, O. Gessner,
 M. Guehr, J. Hajdu, M. P. Hertlein, M. Hoener, O. Ko-
 rnilov, J. P. Marangos, A. M. March, B. K. McFar-
 land, H. Merdji, V. S. Petrović, C. Raman, D. Ray,
 D. Reis, F. Tarantelli, M. Trigo, J. L. White, W. White,
 L. Young, P. H. Bucksbaum, and R. N. Coffee, *Phys.
 Rev. Lett.*, **105**, 083004 (2010).
- ⁶L. Fang, M. Hoener, O. Gessner, F. Tarantelli, S. T.
 Pratt, O. Kornilov, C. Buth, M. Gühr, E. P. Kanter,
 C. Bostedt, J. D. Bozek, P. H. Bucksbaum, M. Chen,
 R. Coffee, J. Cryan, M. Glowonia, E. Kukk, S. R. Leone,
 and N. Berrah, *Phys. Rev. Lett.*, **105**, 083005 (2010).
- ⁷J. M. Glowonia, J. Cryan, J. Andreasson, A. Belkacem,
 N. Berrah, C. I. Blaga, C. Bostedt, J. Bozek, L. F.
 DiMauro, L. Fang, J. Frisch, O. Gessner, M. Gühr,
 J. Hajdu, M. P. Hertlein, M. Hoener, G. Huang, O. Ko-
 rnilov, J. P. Marangos, A. M. March, B. K. McFarland,
 M. H., V. S. Petrovic, C. Raman, D. Ray, D. A. Reis,
 M. Trigo, J. L. White, W. White, R. Wilcox, L. Young,
 R. N. Coffee, and P. H. Bucksbaum, *Opt. Express*, **18**,
 17620 (2010).
- ⁸S. P. Hau-Riege, R. M. Bionta, D. D. Ryutov,
 R. A. London, E. Ables, K. I. Kishiyama, S. Shen,
 M. A. McKernan, D. H. McMahon, M. Messerschmidt,
 J. Krzywinski, P. Stefan, J. Turner, and B. Ziaja, *Phys.
 Rev. Lett.*, **105**, 043003 (2010).
- ⁹G. Doumy, C. Roedig, S.-K. Son, C. I. Blaga, A. D.
 DiChiara, R. Santra, N. Berrah, C. Bostedt, J. D.
 Bozek, P. H. Bucksbaum, J. P. Cryan, L. Fang,
 S. Ghimire, J. M. Glowonia, M. Hoener, E. P. Kan-
 ter, B. Krässig, M. Kuebel, M. Messerschmidt, G. G.
 Paulus, D. A. Reis, N. Rohringer, L. Young, P. Agos-
 tini, and L. F. DiMauro, *Phys. Rev. Lett.*, **106**, 083002
 (2011).
- ¹⁰J. P. Cryan, J. M. Glowonia, J. Andreasson, A. Belka-
 cem, N. Berrah, C. I. Blaga, C. Bostedt, J. Bozek,
 N. A. Cherepkov, L. F. DiMauro, L. Fang, O. Gessner,
 M. Gühr, J. Hajdu, M. P. Hertlein, M. Hoener, O. Ko-
 rnilov, J. P. Marangos, A. M. March, B. K. McFarland,
 H. Merdji, M. Messerschmidt, V. S. Petrović, C. Ra-
 man, D. Ray, D. A. Reis, S. K. Semenov, M. Trigo,
 J. L. White, W. White, L. Young, P. H. Bucksbaum,
 and R. N. Coffee, *J. Phys. B*, **45**, 055601 (2012).
- ¹¹N. Rohringer and R. Santra, *Phys. Rev. A*, **76**, 033416
 (2007).
- ¹²L. S. Cederbaum, F. Tarantelli, A. Sgamellotti, and
 J. Schirmer, *J. Chem. Phys.*, **85**, 6513 (1986).
- ¹³M. Tashiro, M. Ehara, H. Fukuzawa, K. Ueda, C. Buth,
 N. V. Kryzhevoi, and L. S. Cederbaum, *J. Chem.
 Phys.*, **132**, 184302 (2010), [arXiv:1004.3092](https://arxiv.org/abs/1004.3092).
- ¹⁴P. Lablanquie, T. P. Grozdanov, M. Žitnik, S. Car-
 niato, P. Selles, L. Andric, J. Palaudoux, F. Penent,
 H. Iwayama, E. Shigemasa, Y. Hikosaka, K. Soejima,
 M. Nakano, I. H. Suzuki, and K. Ito, *Phys. Rev. Lett.*,
107, 193004 (2011).
- ¹⁵N. Berrah, L. Fang, B. Murphy, T. Osipov, K. Ueda,
 E. Kukk, R. Feifel, P. van der Meulen, P. Salen, H. T.
 Schmidt, R. D. Thomas, M. Larsson, R. Richter, K. C.
 Prince, J. D. Bozek, C. Bostedt, S.-i. Wada, M. N.
 Piancastelli, M. Tashiro, and M. Ehara, *Proc. Natl.
 Acad. Sci. U.S.A.*, **108**, 16912 (2011).
- ¹⁶R. Santra, N. V. Kryzhevoi, and L. S. Cederbaum,
Phys. Rev. Lett., **103**, 013002 (2009).
- ¹⁷W. C. Stolte, Z. X. He, J. N. Cutler, Y. Lu, and
 J. A. R. Samson, *At. Data Nucl. Data Tables*, **69**, 171
 (1998).
- ¹⁸K. Ueda, R. Püttner, N. A. Cherepkov,
 F. Gel'mukhanov, and M. Ehara, *Eur. Phys. J.
 Special Topics*, **169**, 95 (2009).
- ¹⁹K. Siegbahn, C. Nordling, G. Johansson, J. Hedman,
 P. F. Hedén, K. Hamrin, U. Gelius, T. Bergmark, L. O.

- Werme, R. Manne, and Y. Baer, *ESCA applied to free molecules* (North-Holland, American Elsevier, Amsterdam, London, New York, 1969) ISBN 7-204-0160-7.
- ²⁰D. Stalherm, B. Cleff, H. Hillig, and W. Mehlorn, *Z. Naturforsch. Teil A*, **24**, 1728 (1969).
- ²¹W. E. Moddeman, T. A. Carlson, M. O. Krause, B. P. Pullen, W. E. Bull, and G. K. Schweitzer, *J. Chem. Phys.*, **55**, 2317 (1971).
- ²²H. Ågren, *J. Chem. Phys.*, **75**, 1267 (1981).
- ²³R. W. Wetmore and R. K. Boyd, *J. Phys. Chem.*, **90**, 5540 (1986).
- ²⁴Y. H. Jiang, A. Rudenko, M. Kurka, K. U. Kühnel, T. Ergler, L. Foucar, M. Schöffler, S. Schössler, T. Havermeier, M. Smolarski, K. Cole, R. Dörner, S. Düsterer, R. Treusch, M. Gensch, C. D. Schröter, R. Moshhammer, and J. Ullrich, *Phys. Rev. Lett.*, **102**, 123002 (2009).
- ²⁵Y. H. Jiang, T. Pfeifer, A. Rudenko, O. Herrwerth, L. Foucar, M. Kurka, K. U. Kühnel, M. Lezius, M. F. Kling, X. Liu, K. Ueda, S. Düsterer, R. Treusch, C. D. Schröter, R. Moshhammer, and J. Ullrich, *Phys. Rev. A*, **82**, 041403(R) (2010).
- ²⁶J. Als-Nielsen and D. McMorrow, *Elements of modern x-ray physics* (John Wiley & Sons, New York, 2001) ISBN 0-471-49858-0.
- ²⁷A. C. Thompson, J. Kirz, D. T. Attwood, E. M. Gulikson, M. R. Howells, J. B. Kortright, Y. Liu, A. L. Robinson, J. H. Underwood, K.-J. Kim, I. Lindau, P. Pianetta, H. Winick, G. P. Williams, and J. H. Scofield, *X-ray data booklet*, 3rd ed., LBNL/PUB-490 Rev. 3 (Center for X-Ray Optics and Advanced Light Source, Lawrence Berkeley National Laboratory, University of California, Berkeley, California 94720, USA, 2009) xdb.lbl.gov.
- ²⁸See the Data Conservancy for tables of energy levels, fluorescence and Auger decay widths of a multiply-ionized nitrogen atom, and *Mathematica*⁴⁷ files for the models used in this work. For more information on the Data Conservancy, see dataconservancy.org.
- ²⁹B. Nagler, U. Zastra, R. R. Fäustlin, S. M. Vinko, T. Whitcher, A. J. Nelson, R. Sobierajski, J. Krzywinski, J. Chalupsky, E. Abreu, S. Bajt, T. Bornath, T. Burian, H. Chapman, J. Cihelka, T. Döppner, S. Düsterer, T. Dzelzainis, M. Fajardo, E. Förster, C. Fortmann, E. Galtier, S. H. Glenzer, S. Göde, G. Gregori, V. Hajkova, P. Heimann, L. Juha, M. Jurek, F. Y. Khattak, A. R. Khorsand, D. Klinger, M. Kozlova, T. Laarmann, H. J. Lee, R. W. Lee, K.-H. Meiwes-Broer, P. Mercere, W. J. Murphy, A. Przystawik, R. Redmer, H. Reinholz, D. Riley, G. Röpke, F. Rosmej, K. Saksl, R. Schott, R. Thiele, S. Tiggesbäumker, Josef Toleikis, T. Tschentscher, I. Uschmann, H. J. Vollmer, and J. S. Wark, *Nature Phys.*, **5**, 693 (2009).
- ³⁰C. Beylerian and C. Cornaggia, *J. Phys. B*, **37**, L259 (2004).
- ³¹The phenomenological model for N₂ discussed in Ref. 4 is based on molecular rate equations and was designed by Oleg Kornilov and Oliver Gessner.
- ³²A. Szabo and N. S. Ostlund, *Modern quantum chemistry: Introduction to advanced electronic structure theory*, 1st, revised ed. (McGraw-Hill, New York, 1989) ISBN 0-486-69186-1.
- ³³K.-N. Huang, M. Aoyagi, M. H. Chen, B. Crasemann, and H. Mark, *At. Data Nucl. Data Tables*, **18**, 243 (1976).
- ³⁴M. H. Chen, E. Laiman, B. Crasemann, M. Aoyagi, and H. Mark, *Phys. Rev. A*, **19**, 2253 (1979).
- ³⁵M. H. Chen, B. Crasemann, N. Mårtensson, and B. Johansson, *Phys. Rev. A*, **31**, 556 (1985).
- ³⁶I. P. Grant, *J. Phys. B*, **7**, 1458 (1974).
- ³⁷J. H. Scofield, *Phys. Rev. A*, **9**, 1041 (1974).
- ³⁸E. U. Condon and G. H. Shortley, *The theory of atomic spectra* (Cambridge University Press, Cambridge, 1935) ISBN 978-0-521-09209-8.
- ³⁹C. P. Bhalla, *J. Phys. B*, **8**, 2792 (1975).
- ⁴⁰Only single core holes were considered by Bhalla.³⁹ His results need to be averaged over the transitions between multiplets in *LS* coupling scheme to obtain values for electronic configurations.
- ⁴¹M. Crance and M. Aymar, *J. Phys. France*, **46**, 1887 (1985).
- ⁴²M. G. Makris, P. Lambropoulos, and A. Mihelič, *Phys. Rev. Lett.*, **102**, 033002 (2009).
- ⁴³P. W. Milonni and J. H. Eberly, *Laser physics*, 2nd ed. (John Wiley & Sons, Hoboken, New Jersey, 2010) ISBN 978-0-470-38771-9.
- ⁴⁴R. D. Cowan, *The theory of atomic structure and spectra*, Los Alamos Series in Basic and Applied Sciences (University of California Press, Berkeley, 1981) ISBN 978-0520-03821-9.
- ⁴⁵Los Alamos National Laboratory, Atomic Physics Codes, <http://aphysics2.lanl.gov/tempweb/lanl/>.
- ⁴⁶T. Åberg, "Two-photon emission, the radiative Auger effect, and the double Auger process," in *Ionization and transition probabilities*, Atomic Inner-Shell Processes, Vol. 1, edited by B. Crasemann (Academic Press, New York, 1975) pp. 353–375.
- ⁴⁷*Mathematica 8.0*, Wolfram Research, Inc., Champaign, Illinois, USA (2011).
- ⁴⁸A. M. Kondratenko and E. L. Saldin, *Dokl. Akad. Nauk SSSR*, **249**, 843 (1979), [*Sov. Phys. Dokl.* **24**, 986-988 (1979)].
- ⁴⁹R. Bonifacio, C. Pellegrini, and L. M. Narducci, *Opt. Commun.*, **50**, 373 (1984).
- ⁵⁰E. L. Saldin, E. A. Schneidmiller, and M. V. Yurkov, *The physics of free electron lasers* (Springer, Berlin, Heidelberg, New York, 2000) ISBN 3-540-66266-9.
- ⁵¹J. Chalupský, L. Juha, J. Kuba, J. Cihelka, V. Hájková, S. Koptyaev, J. Krása, A. Velyhan, M. Bergh, C. Coleman, J. Hajdu, R. M. Bionta, H. Chapman, S. P. Hau-Riege, R. A. London, M. Jurek, J. Krzywinski, R. Nietubyc, J. B. Pelka, R. Sobierajski, J. Meyer-ter Vehn, A. Tronnier, K. Sokolowski-Tinten, N. Stojanovic, K. Tiedtke, S. Toleikis, T. Tschentscher, H. Wabnitz, and U. Zastra, *Opt. Express*, **15**, 6036 (2007).

- ⁵²A. Barty, R. Soufli, T. McCarville, S. L. Baker, M. J. Pivovarov, P. Stefan, and R. Bionta, *Opt. Express*, **17**, 15508 (2009).
- ⁵³J. Chalupsky, P. Bohacek, V. Hajkova, S. P. Hau-Riege, P. A. Heimann, L. Juha, J. Krzywinski, M. Messerschmidt, S. P. Moeller, B. Nagler, M. Rowen, W. F. Schlotter, M. L. Swiggers, and J. J. Turner, *Nucl. Instr. and Meth. A*, **631**, 130 (2011).
- ⁵⁴S. Moeller, J. Arthur, A. Brachmann, R. Coffee, F.-J. Decker, Y. Ding, D. Dowell, S. Edstrom, P. Emma, Y. Feng, A. Fisher, J. Frisch, J. Galayda, S. Gilevich, J. Hastings, G. Hays, P. Hering, Z. Huang, R. Iversen, J. Krzywinski, S. Lewis, H. Loos, M. Messerschmidt, A. Miahnahri, H.-D. Nuhn, D. Ratner, J. Rzepiela, D. Schultz, T. Smith, P. Stefan, H. Tompkins, J. Turner, J. Welch, B. White, J. Wu, G. Yocky, R. Bionta, E. Ables, B. Abraham, C. Gardener, K. Fong, S. Friedrich, S. Hau-Riege, K. Kishiyama, T. McCarville, D. McMahon, M. McKernan, L. Ott, M. Pivovarov, J. Robinson, D. Ryutov, S. Shen, R. Soufli, and G. Pile, *Nucl. Instr. and Meth. A*, **635**, S6 (2011).
- ⁵⁵R. R. Lucchese, "Molecular photoionization," in *Encyclopedia of Computational Chemistry*, edited by P. v. R. Schleyer (John Wiley & Sons, Chichester, New York, 2005) ISBN 978-0-470-84501-1.
- ⁵⁶H. D. Cohen and U. Fano, *Phys. Rev.*, **150**, 30 (1966).
- ⁵⁷K. Gokhberg, V. Vysotskiy, L. S. Cederbaum, L. Storchi, F. Tarantelli, and V. Averbukh, *J. Chem. Phys.*, **130**, 064104 (2009).
- ⁵⁸The fragmentation probabilities for the two channels in Eq. (10) are deduced from the decay products and probabilities of a SCH in N₂ measured in experiments at third-generation synchrotrons. Namely, the dissociative photoionization cross sections of N₂ for the production of N⁺, N²⁺, N³⁺, and N₂⁺ by one-x-ray-photon absorption have been measured in the photon-energy range from 100 to 800 eV.¹⁷ We use the functional relationship for photon energies above the nitrogen *K*-edge in Table A of Ref. 17 to extrapolate to a photon energy of 1100 eV yielding $\sigma_{N_2^+} = 1.83$ kbarn, $\sigma_{N^+} = 85.0$ kbarn, and $\sigma_{N^{2+}} = 30.4$ kbarn as was used in Refs. 4 and 31 to parametrize the molecular rate equations.
- ⁵⁹A. D. Bandrauk, D. G. Musaev, and K. Morokuma, *Phys. Rev. A*, **59**, 4309 (1999).
- ⁶⁰K. Codling, C. Cornaggia, L. J. Frasinski, P. A. Hatherly, J. Morellec, and D. Normand, *J. Phys. B*, **24**, L593 (1991).
- ⁶¹E. Baldit, S. Saugout, and C. Cornaggia, *Phys. Rev. A*, **71**, 021403 (2005).
- ⁶²The notation in terms of sets indicates that the ordering of i, j and k, l is not relevant as $\tilde{P}_{ij} = \tilde{P}_{ji}$.
- ⁶³S. Düsterer, P. Radcliffe, C. Bostedt, J. Bozek, A. L. Cavalieri, R. Coffee, J. T. Costello, D. Cubaynes, L. F. DiMauro, Y. Ding, G. Doumy, F. Grüner, W. Helml, W. Schweinberger, R. Kienberger, A. R. Maier, M. Messerschmidt, V. Richardson, C. Roedig, T. Tschentscher, and M. Meyer, *New J. Phys.*, **13**, 093024 (2011).
- ⁶⁴T. Pfeifer, Y. Jiang, S. Düsterer, R. Moshhammer, and J. Ullrich, *Opt. Lett.*, **35**, 3441 (2010).
- ⁶⁵S. M. Cavaletto, C. Buth, Z. Harman, E. P. Kanter, S. H. Southworth, L. Young, and C. H. Keitel, "Resonance fluorescence in ultrafast and intense x-ray free electron laser pulses," submitted (2012), arXiv:1205.4918.
- ⁶⁶C. P. Safvan and D. Mathur, *J. Phys. B*, **27**, 4073 (1994).
- ⁶⁷C. Buth, R. Santra, and L. S. Cederbaum, *J. Chem. Phys.*, **119**, 10575 (2003), arXiv:physics/0303100.